Available online at www.sciencedirect.com
ScienceDirect
Journal of Photochemistry and Photobiology A: Chemistry 183 (2006) 126–132
Journal of Photochemistry and Photobiology A:Chemistry
www.elsevier.com/locate/jphotochem

Photochemical synthesis of chlorine gas from iron(III) and chloride solution

M. Lim, K. Chiang, R. Amal *

ARC Centre for Functional Nanomaterials, School of Chemical Engineering and Industrial Chemistry, The University of New South Wales, Sydney 2052, NSW, Australia

Received 5 October 2005; received in revised form 14 February 2006; accepted 5 March 2006
Available online 17 April 2006

Abstract

A new method to produce chlorine gas is presented in this paper. The photo-production of chlorine involves the illumination of an acidified aqueous solution of iron(III) and chloride by UV at 365 nm. This induces a photochemical reduction of iron(III) to iron(II) and the formation of $Cl^{\bullet}$ radicals. The radicals were then rapidly scavenged by the chloride ions to form $Cl_2^{\bullet-}$ which further dissociated to form molecular chlorine. The effects of pH, the initial iron(III) and chloride concentrations, and the preparation of the iron(III) and chloride solutions on the photo-production of chlorine were studied through experiments and numerical modelling. It was found that a combination of 0.5 M iron(III) and chloride ions at a pH value of 1 provided the optimum condition for chlorine photo-production. The amount of chlorine produced decreased at chloride concentrations greater than 500 mM and at pH values above 1. This is attributed to the drop in the concentration of $[Fe(OH)_5Cl]^{2+}$ which is believed to be the main species for $Cl^{\bullet}$ radicals formation as well as the subsequent generation of chlorine gas at different chloride concentrations and pHs.

Keywords: Iron(III); Chloride; Chlorine; UV; Synthesis

1. Introduction

In developing countries, contaminated water is a primary cause of death and illness, killing 1.7 million people, most of whom are children, and bringing disease to an additional 3.3 billion per year [1]. Studies have shown that the disinfection and safe storage of household water by on-site or point-of-use treatment will reduce diarrhoeal and other waterborne diseases in communities and households of both developing and developed countries [2].

Of the several disinfection techniques available, chlorination is the most economical, non-specific disinfection method in water and wastewater treatment. It was one of the first methods used and is still widely employed because of its' effectiveness against a broad spectrum of pathogens; it provides residual protection; and it has well understood operational requirements.

Conventional chlorine synthesis process involves the use of an electrolytic cell and electrolysis, where a non-spontaneous redox reaction, driven to occur by means of electrical energy, converts brine to chlorine gas, caustic soda and hydrogen. Other commercially viable process includes the Deacon's process and its derivative, where gaseous hydrogen chloride reacts with oxygen in the presence of a copper catalyst to form chlorine gas and water [3].

The extent to which chlorination can be used to improve drinking water quality in developing countries depends on a variety of technology-related and site-specific environmental and demographic factors. The electrolysis process, whilst widely applied in developed countries, is impractical in developing countries due to the expertise and energy cost required to operate the electrolysis plant, and the safety hazard arising from the handling of chlorine and hydrogen gases. The Deacon process described previously requires high temperatures, up to 450 °C, and has a corrosive gas feed. Furthermore, the catalytic activity rapidly decreases at elevated temperatures.

Iron(III) ions in aqueous chloride (Cl^-) solution are known to form iron(III) hydroxyl and chloroiron complexes. The relative concentration of the iron(III) complexes is governed by the hydrolysis equilibria shown as reactions (1)–(4), where the values of the equilibrium constants, K, are as reported for solution

* Corresponding author. Tel.: +61 2 9385 4361; fax: +61 2 9385 5966.
E-mail address: R.Amal@unsw.edu.au (R. Amal).

1010-6030/$ – see front matter © 2006 Elsevier B.V. All rights reserved.
doi:10.1016/j.jphotochem.2006.03.005

at pH ≤ 3 and 25 °C [4]:

$$[Fe(OH_2)_6]^{3+} \rightleftharpoons [Fe(OH_2)_5(OH)]^{2+} + H^+, \quad K_1 = 6.5 \times 10^{-3}\,M \tag{1}$$

$$[Fe(OH_2)_6]^{3+} \rightleftharpoons [Fe(OH_2)_4(OH)_2]^{+} + 2H^+, \quad K_2 = 2.1 \times 10^{-6}\,M^2 \tag{2}$$

$$[Fe(OH_2)_6]^{3+} + Cl^- \rightleftharpoons [Fe(OH_2)_5Cl]^{2+} + H_2O, \quad K_3 = 30.2\,M^{-1} \tag{3}$$

$$[Fe(OH_2)_6]^{3+} + 2Cl^- \rightleftharpoons [Fe(OH_2)_4Cl_2]^{+} + 2H_2O, \quad K_4 = 134.9\,M^{-2}. \tag{4}$$

As indicated by the equilibrium equations, the hydrolysis of iron(III) in water is pH dependent. In the absence of Cl^-, $[Fe(OH_2)_6]^{3+}$ is the dominant species at a pH less than 2.5. At higher pHs (>2.5), the equilibrium shifts to the right, resulting in a 50% decrease in the concentration of $[Fe(OH_2)_6]^{3+}$ and an equivalent rise in the concentration of $[Fe(OH_2)_5(OH)]^{2+}$. At pH greater than 5, the $[Fe(OH_2)_6]^{3+}$ species is non-existence and the concentration of $[Fe(OH_2)_5(OH)]^{2+}$ begins to decline with the formation of polynuclear polymers $[Fe_n(OH_2)_x(OH)_m]^{(3n-m)+}$ [5].

In the presence of Cl^- anionic ligand, hydroxy complexes of iron(III), $[Fe(OH_2)_5Cl]^{2+}$ and $[Fe(OH_2)_4Cl_2]^{+}$ coexist at low pHs (<1.0) whilst the $[Fe(OH_2)_5(OH)]^{2+}$ species is only present at a very low level. It has been shown that at the studied Cl^- concentration of 0–2 M, the $[Fe(OH_2)_6]^{3+}$ concentration decreases with an increase in the Cl^- concentration. The concentrations of the $[Fe(OH_2)_5Cl]^{2+}$ and $[Fe(OH_2)_4Cl_2]^{+}$ complexes are also dependent on the Cl^- concentration, with the bulk of the chloroiron complex existing as $[Fe(OH_2)_5Cl]^{2+}$ at Cl^- concentration less than 0.5 M. As more Cl^- are added to the solution, the concentration of $[Fe(OH_2)_5Cl]^{2+}$ begins to drop whilst the $[Fe(OH_2)_4Cl_2]^{+}$ concentration increases [6].

The $[Fe(OH_2)_5(OH)]^{2+}$, $[Fe(OH_2)_5Cl]^{2+}$ and $[Fe(OH_2)_4Cl_2]^{+}$ complexes are photoactive in the ultraviolet and visible spectrum. The charge transfer band of $[Fe(OH_2)_5(OH)]^{2+}$ strongly overlaps the solar UV spectrum (290–400 nm) [7,8], and it photolyses efficiently to produce $[Fe(OH_2)_6]^{2+}$ and $OH^\bullet$ radicals [8,9]:

$$[Fe(OH_2)_5(OH)]^{2+} + H_2O \xrightarrow{h\nu} [Fe(OH_2)_6]^{2+} + OH^\bullet, \quad k_5^+ = I\phi_5. \tag{5}$$

Likewise, $[Fe(OH_2)_5Cl]^{2+}$ and $[Fe(OH_2)_4Cl_2]^{+}$ photolyse in the charge-transfer band at 270–400 nm to form $[Fe(OH_2)_6]^{2+}$ and $Cl^\bullet$:

$$[Fe(OH_2)_5Cl]^{2+} + H_2O \xrightarrow{h\nu} [Fe(OH_2)_6]^{2+} + Cl^\bullet, \quad k_6^+ = I\phi_6 \tag{6}$$

$$[Fe(OH_2)_4Cl_2]^{+} + H_2O \xrightarrow{h\nu} [Fe(OH_2)_5Cl]^{+} + Cl^\bullet, \quad k_7^+ = I\phi_7. \tag{7}$$

The rate constants, k_n^+ (where $n = 5$, 6 and 7), for the forward reaction for reaction (5)–(7) are given by the product of the rate of incident radiation upon the reactor, I, and the quantum yields, ϕ_n (where $n = 5$, 6 and 7), of each photolysis reactions. The quantum yield is defined as the mole of reactant consumed or product formed per mole of photon absorbed.

Reviews by Feng and Nansheng [5] and Nadtochenko and Kiwi [6] revealed that a variety of techniques such as laser kinetic spectroscopy [6], monitoring the reduction of iron(III) [8], alcohol scavenging [9–11], iron isotope exchanges between the two oxidation states [12], and radical-initiated polymerizations [13,14] had been used to determine the primary quantum yields of reaction (5). Quantum yields of $OH^\bullet$ and $[Fe(OH_2)_6]^{2+}$, ranging from 0.07 to 0.31 and from 0.067 to 0.29, respectively, were reported for measurements at wavelengths between 253.7 and 365 nm. Differences in the measurement technique may account for the range of quantum yield obtained in literature.

For the photo-dissociation of $[Fe(OH_2)_5Cl]^{2+}$, quantum yields of between 0.093 and 0.13 were measured in photopolymerisation studies and steady-state photolysis using *tert*-butyl alcohol as the scavenger at wavelengths ranging from 300 to 400 nm [10,15–19]. Other investigators [6] have found higher quantum yield values in the range of 0.46–0.57 from laser kinetic spectroscopy measurements. They attributed the lower quantum yield values obtained from conventional steady-state technique to interference from secondary radical reactions during the measurement process. For example, the $Cl^\bullet$ radical will react with ferrous photochemical products in a radical termination reactions, resulting in a lower measured quantum yield.

The $OH^\bullet$ and $Cl^\bullet$ radicals formed from the photo-dissociation reactions are rapidly scavenged by the Cl^- ions to form $Cl_2^{\bullet-}$ and $ClOH^{\bullet-}$ [6,20]:

$$Cl^\bullet + Cl^- \rightleftharpoons Cl_2^{\bullet-}, \quad k_8^+ = 2.0 \times 10^{10}\,M^{-1}\,s^{-1}, \quad k_8^- = 1.1 \times 10^5\,s^{-1} \tag{8}$$

$$OH^\bullet + Cl^- \rightleftharpoons ClOH^{\bullet-}, \quad k_9^+ = 4.3 \times 10^9\,M^{-1}\,s^{-1}, \quad k_9^- = 6.1 \times 10^9\,s^{-1}. \tag{9}$$

Some work has suggested that $Cl_2^{\bullet-}$ formed will further disproportionate to form molecular chlorine, implying that Cl_2 (at pH < 3) or HClO (at pH > 3) is the final stable product [6,20]:

$$Cl_2^{\bullet-} + Cl_2^{\bullet-} \rightarrow Cl_3^- + Cl^-, \quad k_{10}^+ = 3.1 \times 10^9\,M^{-1}\,s^{-1} \tag{10}$$

$$Cl_3^- \rightleftharpoons Cl_2 + Cl^-, \quad k_{11}^+ = 1.8 \times 10^{-1}\,M^{-1}. \tag{11}$$

$[Fe(OH_2)_6]^{2+}$ will also react rapidly with the $OH^\bullet$ and $Cl^\bullet$ radicals according to reaction (12) and (13). However, for high (0.5 M) chloride concentration solutions, the Cl^- ions will compete with $[Fe(OH_2)_6]^{2+}$ for these radical intermediates [20]:

$$Cl^\bullet + [Fe(OH_2)_6]^{2+} \rightarrow Cl^- + [Fe(OH_2)_6]^{3+}, \quad k_{12}^+ = 5.9 \times 10^9\,M^{-1}\,s^{-1} \tag{12}$$

$$OH^{\bullet} + [Fe(OH_2)_6]^{2+} \rightarrow OH^- + [Fe(OH_2)_6]^{3+},$$
$$k_{13}^{+} = 2.3 \times 10^8\ M^{-1}\ s^{-1}. \quad (13)$$

The $[Fe(OH_2)_6]^{2+}$ may also react directly with the $Cl_2^{\bullet -}$ species. However, at the onset of irradiation, the reaction between $[Fe(OH_2)_6]^{2+}$ and $Cl_2^{\bullet -}$ is probably too slow to out compete the $Cl_2^{\bullet -}$ disproportionation reaction. Nonetheless, $[Fe(OH_2)_6]^{2+}$ may become a sink for $Cl_2^{\bullet -}$ as $[Fe(OH_2)_6]^{2+}$ concentrations increase over the course of the irradiation [20]:

$$Cl_2^{\bullet -} + [Fe(OH_2)_6]^{2+} \rightarrow 2Cl^- + [Fe(OH_2)_6]^{3+},$$
$$k_{14}^{+} = 1.4 \times 10^7\ M^{-1}\ s^{-1}. \quad (14)$$

This paper describes a new method which has been developed to produce chlorine for the purpose of water disinfection. It involves exposing an aqueous solution containing iron(III) and Cl^- ions at pH less than or equal to 2.0 to UV light. The effects of iron(III) concentration, Cl^- concentration and pH on chlorine generation are investigated by laboratory experiments coupled with numerical modelling with the aim to understand and optimise the chlorine generation process.

2. Experimental

2.1. Reactor Setup

The effects of pH, and the initial iron(III) and Cl^- concentrations on the chlorine generation process were studied using a laboratory scale reactor (Fig. 1). The coil reactor (1) is fabricated from high purity grade quartz (5.0 mm inside diameter, 6.0 mm outside diameter) for maximum transmission of UV and visible light. The reactor was mounted vertically on a support and a 20 W blacklight fluorescent lamp (NEC, emission range 300–400 nm, maximum emission at 365 nm), attached to a domestic lamp holder, was fitted through the centre of the reactor. The reactor was connected to a gas–liquid separator (2) and a gas trap (3) by means of Masterflex® flexible tubings. The solution containing iron(III) and chloride ions was introduced into the reactor at the injection port (4) and a Masterflex® Quick Load peristaltic pump (5) was used to circulate the solution in the loop.

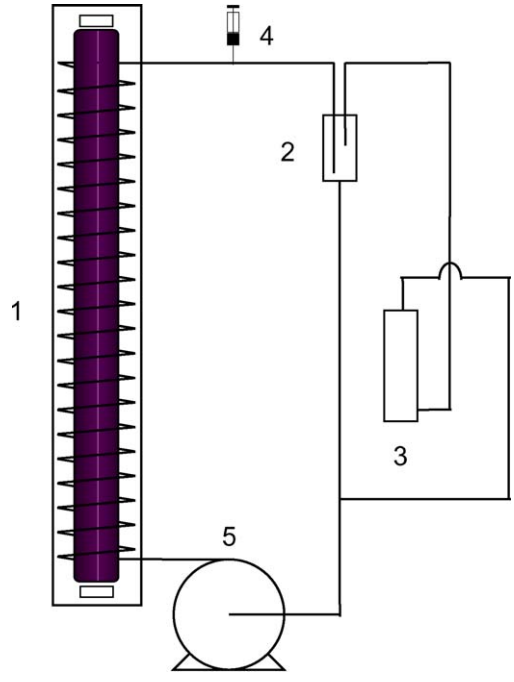

Fig. 1. Schematic diagram of the spiral reactor showing the coil reactor (1), gas–liquid separator (2), gas trap (3), injection port (4) and Masterflex® Quick Load peristaltic pump (5).

In a typical photolysis reaction, the reactor was charged with a 50 ml aliquot of freshly prepared iron(III) and Cl^- solution. The solution was irradiated by the UV lamp as it flowed through the spiral reactor, resulting in the production of chlorine gas. Separation of the gas and liquid phases occurred in the gas–liquid separator. Chlorine gas was collected by passing the gas phase through a 10 mM NaOH solution in the gas trap. Gas leaving the trap's outlet was returned back to the spiral reactor.

The generation of Cl_2 gas under different pH values, and iron(III) and Cl^- concentrations was followed by measuring the amount of chlorine in the gas trap after a period of 1 h. As the amount of Cl_2 generated increased, the amount of Cl_2 gas dissolved in the NaOH solution gas trap increased and resulted in an increase of chlorine concentration. The chlorine concentration was then determined by UV–vis spectroscopic analysis with *N*,*N*-diethyl-*p*-phenylenediamine sulfate (DPD) as the indicator [21].

2.2. Actinometry studies

Ferrioxalate actinometry was performed according to the protocol of Hatchard and Parker [22] in order to determine the amount of photons absorbed by the solution inside the reactor. Photolytic production of Fe(II) was limited to <10% of the initial iron(III) to insure maximum photon absorption by the ferrioxalate actinometer. A quantum yield of 1.23 at 365 nm for ferric oxalate photolysis was used in the calculation [22].

2.3. Effects of pH

Solutions containing 100 mM of iron(III) and 100 mM of Cl^- ions were prepared by mixing 4.04 g $Fe(NO_3)_3{\cdot}9H_2O$ with 5 ml of 2 M NaCl in a 100 ml volumetric flask and diluting to the mark with deionised-distilled water. This solution mixture had a pH value of 1.6 prior to pH adjustment which could be adjusted to lower and higher values by adding $HClO_4$ and NaOH, respectively.

2.4. Effects of iron(III) and chloride concentrations

Aqueous solutions containing different ratios of iron(III) (100–500 mM) and Cl^- ions (50–1000 mM) were prepared as described below. The required amount of $Fe(NO_3)_3{\cdot}9H_2O$ was dissolved in 50 ml of deionised water that has been mixed with the required volume (up to 50 ml) of 2 M NaCl. The solutions containing iron(III) species and Cl^- ions were then diluted to a

final volume of 100 ml in a volumetric flask and acidified to pH 1.0 by adding a few drops of 70% $HClO_4$.

2.5. Speciation of iron(III)

The speciation of iron(III) in the presence of Cl^- ions, and at different pH values was studied through experiments and numerical modelling. In the experimental studies, the amount of chlorine produced from the photolysis of two solutions containing equal concentration of iron(III) and Cl^- ions, but prepared using different precursors, was measured. The first solution was prepared by mixing 20.2 g of $Fe(NO_3)_3{\cdot}9H_2O$ and 75 ml of 2 M NaCl with 25 ml of deionised-distilled water. The second solution was prepared by mixing 13.5 g of $FeCl_3{\cdot}6H_2O$ and 75 ml of 2 M $Na(NO_3)_3$ with 25 ml of deionised-distilled water.

2.6. Kinetic studies

Kinetic studies were also undertaken by monitoring the iron(II) concentrations in the reactor, and the chlorine concentration in the gas trap over time. The iron(II) concentration was determined spectroscopically using *o*-phenanthroline as the indicator [21].

2.7. Numerical modelling

Numerical simulations were conducted using PHREEQC Version 2.10, a hydrogeochemical modelling software package [4]. The simulation were carried out for aqueous solutions containing 100, 250 or 500 mM of iron(III) species and Cl^- concentrations ranging between 50 and 1000 mM.

The data provided in PHREEQC's database were used to calculate the equilibrium concentrations of each species before a kinetic calculation was initiated, and again when a kinetic reaction increment was added. A set of rate expressions were derived for reactions (5)–(14) and integrated with an embedded fourth and fifth order Runge-Kutta-Fehlberg algorithm. The rate constant for reactions (8)–(14) was taken from literature as shown in the previous section. The rate constants for reaction (5)–(7) are given by the product of the amount of radiation incident upon the reactor, I, and the quantum yields, ϕ_n (where $n = 5$, 6 and 7), of each photolysis reactions. The value of I was obtained from the actinometry experiments. The value of ϕ_5, ϕ_6 and ϕ_7, were not measured in this work. Nadtochenko and Kiwi [6] reported the values of ϕ_5 and ϕ_6 to be 0.24 ± 0.06 and 0.47 ± 0.11, respectively, and these values were used in the calculations. The value of ϕ_7 has not been published and is assumed to be negligible.

3. Results and discussion

3.1. Equilibrium speciation at different iron(III) and Cl^- concentrations

The results of the simulations showed that in the presence of iron(III) and Cl^- ions at pH 1, The $[Fe(OH_2)_6]^{3+}$, $[Fe(OH_2)_5(OH)]^{2+}$, $[Fe(OH_2)_5Cl]^{2+}$ and $[Fe(OH_2)_4Cl_2]^+$ are the dominant species in the solution. The equilibrium concentrations of these species for a 500 mM iron(III) solution at pH 1.0 and various Cl^- concentrations are shown in Fig. 2. These figures show that for the same Cl^- concentration, the relative concentrations of each species increase with increasing iron(III) concentration. In the absence of Cl^- ions, $[Fe(OH_2)_6]^{3+}$ is the dominant species at pH 1.0. In the presence of the Cl^- ions, $[Fe(OH_2)_6]^{3+}$, $[Fe(OH_2)_5Cl]^{2+}$ and $[Fe(OH_2)_4Cl_2]^+$ coexist. At the studied range of total Cl^- concentration between 0 and 2 M, the $[Fe(OH_2)_6]^{3+}$ concentration decreases with an increase in Cl^- concentration. The concentrations of $[Fe(OH_2)_5Cl]^{2+}$ and $[Fe(OH_2)_4Cl_2]^+$ complexes are also dependent on the Cl^- concentration, with the bulk of the chloroiron complex existing as $[Fe(OH_2)_5Cl]^{2+}$ at concentration less than 0.5 M. As more Cl^- ions are added to the solution, the concentration of $[Fe(OH_2)_5Cl]^{2+}$ begins to drop whilst the $[Fe(OH_2)_4Cl_2]^+$ concentration increases. These results are consistent with those reported by Nadtochenko and Kiwi [6].

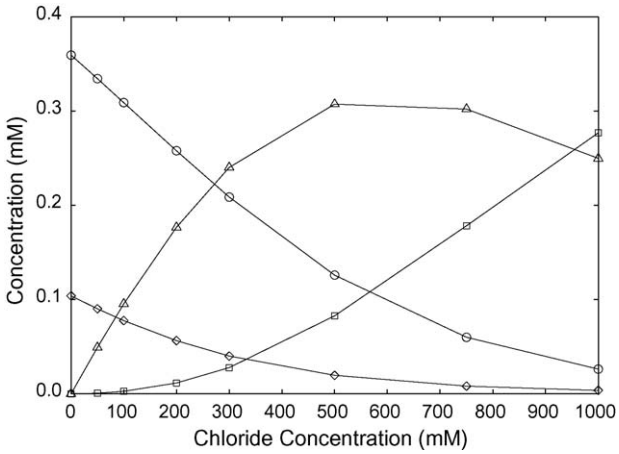

Fig. 2. Equilibrium $[Fe(OH_2)_6]^{3+}$ (◯), $[Fe(OH_2)_5Cl]^{2+}$ (△), $[Fe(OH_2)_4Cl_2]^+$ (□) and $[Fe(OH_2)_5(OH)]^{2+}$ (◇) concentrations in a 500 mM iron(III) solution at pH of 1.0 and various Cl^- concentration as calculated by PHREQQC.

3.2. Chlorine generated at different iron(III) and Cl^- concentrations

The rate of photons absorbed by the solution was determined by ferric oxalate actinometry to be 50 $\mu E\, l^{-1}\, s^{-1}$. No measurable chlorine and changes in the iron(III) concentration was detected in dark control experiments.

Fig. 3 shows the amount of chlorine in the gas trap measured experimentally after 1 h of UV illumination, at this photon absorption rate, as a function of Cl^- concentration for different initial concentrations of iron(III) and Cl^- ions, at pH 1.0, in the reactor. A slight drop in pH, from 1.0 to 0.8 ± 0.1, was observed at the end of the experiment. The uncertainty in the chlorine concentration measurements, which arises from the collection technique used and the dilution of the sample solution prior to analysis, was estimated to be ±10%.

Fig. 4 shows the simulated results obtained from the PHREEQC modelling package. Overall, the simulated results are comparable to those obtained experimentally with the exception of chlorine produced at Cl^- concentration less than

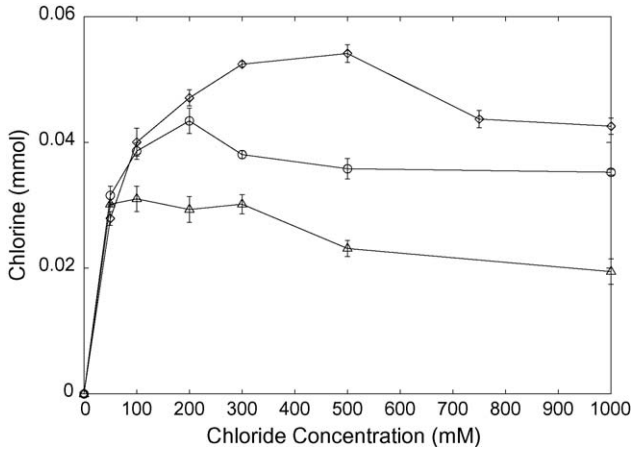

Fig. 3. Amount of chlorine in the gas trap after 1 h as produced by 100 mM (△), 250 mM (◯) and 1000 mM (◊) iron(III), for Cl^- concentration between 50 and 1000 mM.

100 mM. The difference between the simulated and measured results is attributed to uncertainty in the chlorine detection technique, especially at a low chlorine concentration. The amount of chlorine produced was shown to increase with increasing total Cl^- concentration and at higher iron(III) concentration. However, when the Cl^- concentration exceeded 500 mM, a slight drop in the photo-production of chlorine was observed for all three iron(III) concentrations. This observation can be explained by the fact that the key iron complex responsible for the $Cl^\bullet$ radical formation, and thus chlorine generation, is $[Fe(OH_2)_5Cl]^{2+}$. An inspection of the thermodynamic calculation (Fig. 2) reveals that the $[Fe(OH_2)_5Cl]^{2+}$ concentration increases with the increase in the Cl^- concentration for Cl^- concentrations less than 500 mM, thus resulting in more chlorine being produced. As more Cl^- ions are added to the solution (>500 mM), the formation of $[Fe(OH_2)_4Cl_2]^+$ is more favourable, resulting in a drop in the $[Fe(OH_2)_5Cl]^{2+}$. Consequently a reduction in the amount of chlorine gas produced is observed. The reasonable comparison between the simulated and experimental results also suggests that the assumption of ϕ_7 being significantly less than that of ϕ_6 is valid.

When the amount of chlorine produced at the end of 1 h from the photolysis of solutions containing equal concentration of ions, that is 0.5 M iron(III), 1.5 M Cl^- and 1.5 M NO_3^-, was compared, the solution prepared from iron (III) nitrate and sodium chloride was found to produce 0.033 ± 0.001 mmol chlorine in the gas trap whereas solution prepared from iron (III) chloride and sodium nitrate produced 0.020 ± 0.001 mmol. The difference can be explained by the fact that in solution prepared by mixing iron (III) nitrate with sodium chloride, the probability of one Fe^{3+} ions being coordinated with more than one Cl^- ion is relatively small [23]. Thus, it is likely that $[Fe(OH_2)_5Cl]^{2+}$ is the dominant complex in this system. Whereas, a freshly prepared solution of iron (III) chloride will contain the species $[Fe(OH_2)_6]^{3+}$, $[Fe(OH_2)_5Cl]^{2+}$, $[Fe(OH_2)_4Cl_2]^+$, $[Fe(OH_2)_3Cl_3]$, $[Fe(OH_2)_2Cl_4]^-$, $[Fe(OH_2)Cl_5]^{2-}$ and $[FeCl_6]^{3-}$ [23]. The fact that more chlorine gas is generated in the former supports our hypothesis that the $[Fe(OH_2)_5Cl]^{2+}$ is the primary source of chlorine radical when the solution was photolysed, and is thus the key complex responsible for producing molecular chlorine. The different yield of Cl_2 gas observed by using different iron(III) precursors is interesting and warrants further investigation.

3.3. Kinetic studies

The amount of molecular chlorine produced and the change in the amount of iron(II) in the reactor with reaction time are shown in Figs. 5 and 6, respectively. At the end of 6 h, the pH dropped slightly from 1.0 to 0.8 ± 0.1. Fig. 5 shows a high initial chlorine production rate which subsequently decreases with time. This is likely due to the concurrent increase in iron(II) concentration as the result of photo-reduction of iron(III) in the solution. The iron(II) will react with molecular chlorine, as described by Eqs. (12) and (14), thus reducing the amount chlorine produced.

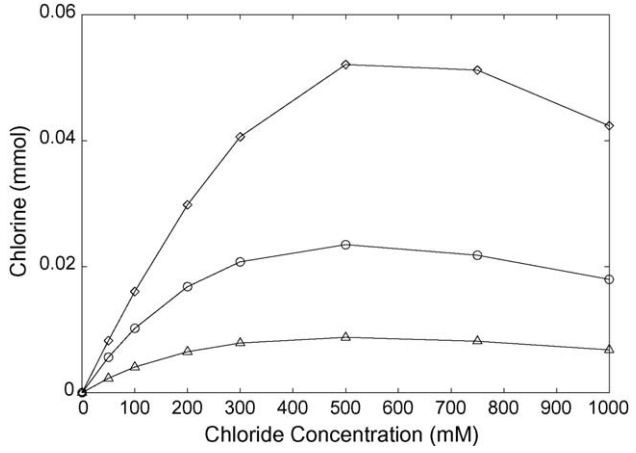

Fig. 4. Amount of chlorine produced after 1 h, by 100 mM (△), 250 mM (◯) and 1000 mM (◊) iron(III), for Cl^- concentration between 50 and 1000 mM, as simulated by PHREEQC.

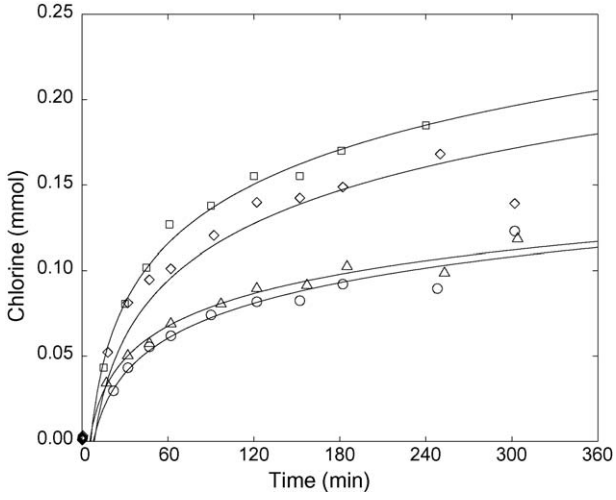

Fig. 5. Amount of chlorine produced by 100 mM iron(III) and 50 mM Cl^- ions (△); and 500 mM iron(III) and 50 mM (◯), 500 mM (□) and 1000 mM (◊) Cl^- ions.

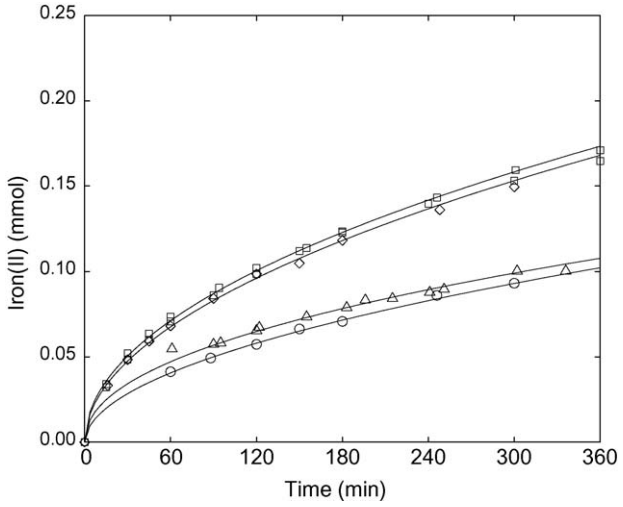

Fig. 6. Amount of iron(II) produced from the photolysis of 100 mM iron(III) and 50 mM Cl^- ions (△); and 500 mM iron(III) and 50 mM (◯), 500 mM (□) and 1000 mM (◊) Cl^- ions.

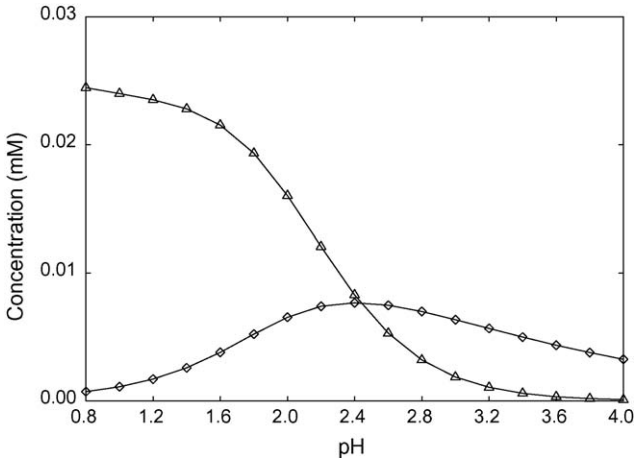

Fig. 8. $[Fe(OH_2)_5Cl]^{2+}$ (△) and $[Fe(OH_2)_5(OH)]^{2+}$ (◊) concentration in 100 mM of iron(III) and Cl^- solution at different pH, as simulated by PHREEQC.

The figures also show that at the end of 6 h, the amount of iron(II) formed is roughly equal to the amount of chlorine formed for all iron(III) and Cl^- concentration investigated. When the Cl^- concentration was increased beyond iron(III) to Cl^- ratio of 1:1, the chlorine production rate begins to drop due to a shift of the equilibrium towards less $[Fe(OH_2)_5Cl]^{2+}$, and more $[Fe(OH_2)_4Cl_2]^+$, as has been discussed previously.

3.4. Effects of pH

Fig. 7 shows the amount of generated chlorine in the gas trap after illuminating 100 mM of iron(III) and 100 mM of Cl^- for 1 h as a function of pH. The results show that more chlorine is produced at a low pH value of 1.0–1.3, and no detectable amount of chlorine is produced at pH greater than 2.0. A slight drop in pH (<0.2) from the initial pH value was also observed at the end of the experiments.

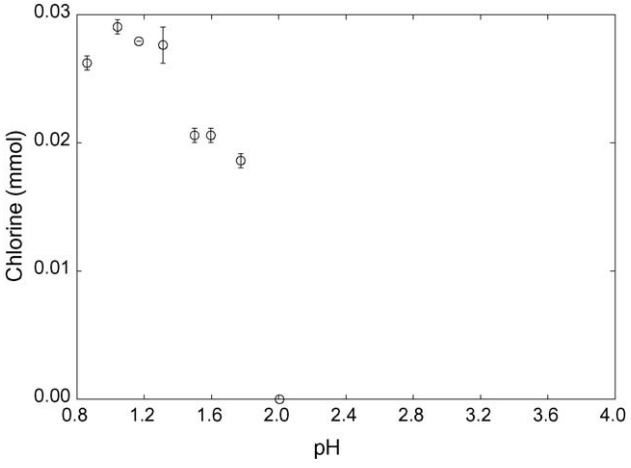

Fig. 7. Amount of chlorine in the gas trap after 1 h of UV illumination, as a function of pH in the reactor.

The decrease in chlorine production with the increase in solution pH is most likely due to changes in the dominant iron(III) species with pH. Fig. 8 shows the $[Fe(OH_2)_5Cl]^{2+}$ and $[Fe(OH_2)_5(OH)]^{2+}$ concentration as a function of pH, calculated by the PHREEQC modelling. The figure reveals that at low pH the iron speciation is dominated by $[Fe(OH_2)_5Cl]^{2+}$ which will undergo photolysis to form $Cl^\bullet$ radicals. The $Cl^\bullet$ radicals are scavenged by Cl^- ions, leading to the formation of $Cl_2^{\bullet -}$, and eventually molecular chlorine, Cl_2. With increase in pH, the equilibrium shifted towards the formation of more $[Fe(OH_2)_5(OH)]^{2+}$ and a drop in the concentration of the $[Fe(OH_2)_5Cl]^{2+}$ complex. This in turn results in less $Cl^\bullet$ being produced and consequently, less chlorine being generated. While some researchers have suggested that the scavenging of $OH^\bullet$ radicals, produced from the photolysis of $[Fe(OH_2)_5(OH)]^{2+}$, by Cl^- ions will form $ClOH^-$, leading eventually to the formation of HClO at pH 3 [20], later investigation involving pulsed laser spectroscopy [6] showed that the concentration of $ClOH^-$ is very low ($\sim 10^{-8}$ M) at both pH 0.95 and 1.92. This suggested that negligible amount of chlorine is produced via the scavenging of $OH^\bullet$ radicals by Cl^- ions.

The drop in the amount of chlorine produced can also be explained by the pH dependent speciation of chlorine in aqueous solution. Previous investigators have reported that that at low pH (<1), an appreciable amount of chlorine exists as molecular chlorine in the solution while a pH between 4 and 7 favours the formation of hypochlorous acid [3]. Molecular chlorine, which has a Henry constant of 9.5×10^{-2} M atm^{-1} [24], is easily expelled from the solution as chlorine gas whereas, hypochlorous acid, with a Henry constant of 6.6×10^2 M atm^{-1} [25], tends to remain in solution. In order to confirm that the small amount of chlorine gas detected in the gas trap at pH 2 or greater is not due to the difficulty in expelling Cl_2 gas from the solution at high pH, the solution pH was reduced from 2.0 to 1.0 by adding a few drops of 70% $HClO_4$ at the end of the photolysis experiment. The solution was then circulated within the reactor in the dark. In principle, lowering the pH will shift the equilib-

rium such that any hypochlorous acid dissolved in the solution will be converted to molecular chlorine and expelled from the solution. No chlorine gas was detected in the gas trap after 1 h of purging confirming the lack of generation of chlorine in the reactor.

4. Conclusion

The generation of chlorine gas from the UV irradiation of aqueous iron(III) and Cl^- solution at 365 nm was found to depend on Cl^- concentration and pH of the solution.

The amount of chlorine produced increased with increasing Cl^- concentration, and more chlorine was produced at higher iron(III) concentration. However, when the iron(III) to Cl^- concentration ratio was greater than 1, a slight drop in the amount of chlorine produced was observed. This suggests that $[Fe(OH_2)_5Cl]^{2+}$ is the active light absorber species and the photolysis of $[Fe(OH_2)_4Cl_2]^+$ is insignificant. A low pH value (<1.0) also favours the formation of chlorine gas whilst no detectable amount of chlorine was produced at pH greater than 2.0. The later is mainly due to a shift in the equilibrium towards the formation of more $[Fe(OH_2)_5(OH)]^{2+}$, and less $[Fe(OH_2)_5Cl]^{2+}$ complexes.

Advantageously, the chlorine generation process described in this work does not involve electrolysis and therefore can be carried out without the provision of electrical energy. Since the main requirements for the reaction are iron(III), Cl^- and UVA irradiation, the process has the potential to utilise scrap iron, sea water and solar energy—materials and energy sources that are widely and cheaply available in developing countries. It is of low cost, relatively safe and simple to maintain. It also has the potential of operating cyclically with regeneration of the raw material, thus reducing the need for waste disposal. In conclusion, the process described has the potential of being a low cost and effective method of disinfecting water in developing countries.

References

[1] World Health Organisation, The World Health Report 2002, Geneva, 2002.
[2] T. Thompson, M. Sobsey, J. Bartram, Int. J. Environ. Health Res. Suppl. 13 (2003) S89.
[3] G.C. White, Handbook of Chlorination, Van Nostrand Reinhold Company, New York, 1972.
[4] D.L. Parkhurst, C.A.J. Appelo, User's Guide To PHREEQC (Version 2)—A Computer Program For Speciation, Batch-Reaction, One-Dimensional Transport, And Inverse Geochemical Calculations, Water-Resources Investigations Report 99-4259, U.S. Geological Survey Central Region Research, Denver, 1999.
[5] W. Feng, D. Nansheng, Chemosphere 41 (2000) 1137.
[6] V.A. Nadtochenko, J. Kiwi, Inorg. Chem. 37 (1998) 5233.
[7] C.J. Weschler, M.L. Mandich, T.E. Graedel, J. Geophys. Res. D: Atmos. 91 (1986) 5189.
[8] B.C. Faust, J. Hoigné, Atmos. Environ. 24A (1990) 79.
[9] J.H. Baxendale, J. Magee, Trans. Faraday Soc. 51 (1955) 205.
[10] C.H. Langford, J.H. Carey, Can. J. Chem. 53 (1975) 2430.
[11] H.J. Benkelberg, P. Warneck, J. Phys. Chem. 99 (1995) 5214.
[12] A.W. Adamson, W.L. Waltz, E. Zinato, D.W. Watts, P.D. Fleischauer, R.D. Lindholm, Chem. Rev. 68 (1962) 541.
[13] M.G. Evans, N. Uri, Nature (1949) 404.
[14] H.G.C. Bates, N. Uri, J. Am. Chem. Soc. 51 (1953) 2754.
[15] V. Balzani, V. Carassiti, Photochemistry of Coordination Compounds, Academic Press, New York, 1970.
[16] M.G. Evans, M. Santappa, N. Uri, J. Polym. Sci. 7 (1951) 243.
[17] F. David, P.G. David, J. Phys. Chem. 80 (1976) 1090.
[18] S.R. Palit, P. Ghosh, J. Polym. Sci. 58 (1962) 1225.
[19] M.K. Saha, P. Ghosh, S.R. Palit, J. Polym. Sci. A2 (1964) 1365.
[20] D.W. King, R.A. Aldrich, S.E. Charnecki, Mar. Chem. 44 (1993) 105.
[21] American Water Works Association, Standard Methods for the Examination of Water and Wastewater, American Public Health Association, American Water Works Association and Water Environment Federation, Washington, DC, 1998.
[22] C.G. Hatchard, C.A. Parker, Proc. R. Soc. Lond. A235 (1956) 518.
[23] E. Rabinowitch, W.H. Stockmayer, J. Am. Chem. Soc. 64 (1942) 335.
[24] D.R. Lide, H.P.R. Frederikse, CRC Handbook of Chemistry and Physics, CRC Press Inc., Boca Raton, Florida, 1995.
[25] T. Huthwelker, S.L. Clegg, T. Peter, K. Carslaw, B.P. Luo, P. Brimblecombe, J. Atmos. Chem. 21 (1995) 81.